Cell and Tissue Research (2019) 376:309–323
https://doi.org/10.1007/s00441-019-02992-1

REGULAR ARTICLE

Histoarchitecture restoration of cerebellar sub-layers as a response to estradiol treatment following Kainic acid-induced spinal cord injury

Amany Farag[1] · S. Lashen[1] · R. Eltaysh[2]

Received: 24 June 2018 / Accepted: 29 December 2018 / Published online: 20 February 2019

Abstract

One of the major impacts of spinal cord injury (SCI) is the cerebellar neurological malfunction and deformation of its sub-layers. This could be due to the enormous innervation of the spinocerebellar tract from the posterior gray horn in the spinal cord to the ipsilateral cerebellum. Although the neuroprotective role of estradiol in spinal cord (SC) injuries, as well as its ability to delay secondary cell death changes, is well-known, its effect on cerebellar layers is not fully investigated. In this study, a SCI model was achieved by injection of Kainic acid into SC of adult Male Wistar rats in order to assess the effects of SCI on the cerebellum. The animals were classified into SCI group (animals with SCI), estradiol-treated group (animals with SCI and received estradiol), control groups, and sham control group. The microscopical examination 24 h after induction of SCI revealed that KA induced the most characteristics of neurodegeneration including astrocytic propagation and microglial activation. The estradiol was injected intraperitoneally 20 min after induction of SCI, and the samples were collected at 1, 3, 7, 14, and 30 days. Histologically, the estradiol reduced the inflammatory response, enhanced the recovery of molecular, granular, and Purkinje cell layers, and therefore aided in the restoration of layer organization. These findings were also confirmed by immunohistochemical staining and gene expression profiling.

Keywords Cerebellum · Spinal cord injury · Estrogen · Kainic acid · Astrocytes · GFAP

Abbreviations

SCI	Spinal cord injury
SC	Spinal cord
KA	Kainic acid
IP	Intraperitoneal
ROS	Reactive oxygen species
IHC	Immunohistochemistry
CSF	Cerebrospinal fluid
PBS	Phosphate buffer saline

Introduction

Although the side effects that emerge from the injury of spinal cord in terms of loss of motor or sensory functions are always referred to injury on the spinal cord itself, these malfunctions could also be a consequence of cerebellar-composition damage which lead to alterations of body balance, movement coordination, and motor learning (Wolf et al. 2009). These alterations can be interpreted by varied apoptotic pathways triggered after SCI that correlate with inflammatory cascades initiation and neurological degeneration to cerebellar layers (Mills et al. 2000). The correlation between the spinal cord and the cerebellum has been described in the light of integrated relationship, whereas cerebellum plays a fundamental part in handling proprioceptive information that is mandatory for coordinating ongoing voluntary movement (Gulgun et al. 2015). The neurotransmissions traced from Clarke's nucleus axons in SC are shifted inside dorsal tract to cerebellar lobules under the name of mossy fibers to innervate the granular layer cells. These cells transmit signals to parallel fibers that deliver precise afferent inputs to distal portions of Purkinje cell dendrites, while the proximal dendrites are straightly stimulated

✉ Amany Farag
vetdramany@yahoo.com; amanyfarag@mans.edu.eg

[1] Department of Cytology and Histology, Faculty of Veterinary Medicine, Mansoura University, Gomhoria St., P.O. box 35516, Mansoura, Egypt

[2] Department of Pharmacology, Faculty of Veterinary Medicine, Mansoura University, Gomhoria St., P.O. box 35516, Mansoura, Egypt

by an excitatory climbing fiber that originates from the olive nucleus in the brainstem (Stacey et al. 2013). Purkinje cells manage the circuitry of the cerebellum by processing the neuronal activity and the fine-adjustment of the afferent circuitry of the molecular zone (Joshua et al. 2014). From these points but also depending on our observations that spotted a huge influence on body behavioral functions, the cerebellum was selected as a target object to evaluate the effect of treatment in this study. During tracing the consequences of SCI, an intensive collateral damage of cerebellar sub-layers and an elevated level in the concentration of extracellular glutamate are spotted. This glutamate is considered as one of the excitatory neurotransmitters released by 40% of all synapses (Coyle and Puttfarcken 1993) to play a crucial role in neural signaling pathways, differentiation, and neuro-plasticity. The elevated level of glutamate is accused as one of the factors responsible for neuronal excitotoxicity (Mills et al. 2000). To confirm this hypothesis and mimic glutamate's effect in inducing neuronal apoptosis, a selective glutamate receptor agonist as Kainic acid (KA) has been commonly used (Drexel et al. 2012). Kainic acid was initially used as an anthelmintic composite for gastrointestinal worms after its extraction and characterization from the seaweed (Murakami et al. 1953). Subsequent study, created by Sperk (1994), has reported Kainic acid excitotoxic potency in CNS with induction of neuropathological and inflammatory changes. Later on, these neuroexcitotoxic-driven inflammatory changes were traced to interacted activated kainate receptors (KARs) termed as one subtype of ionotropic glutamate receptors (iGluRs). Provoking of these iGluRs is correlated with intracellular calcium augmentation that motivates the excessive release of free radicals like reactive oxygen species (ROS), the mediators of oxidative stress (Bruce and Baudry 1995). This promotes an imbalance between free radicals' production and antioxidants leading to oxidation of membrane elements that is followed by mitochondrial dysfunction and ultimately results in cellular apoptosis and death. The disturbance in glutamate level not only causes neural transmission failure but also initiates excitotoxicity that is involved in a various type of neurodegenerative diseases like Alzheimer where the selective destructive effect of KA to pyramidal cells of the hippocampus is proven (Nadler et al. 1978). KA is considered a dose-dependent agent where low doses led to nuclei pyknosis with nucleolus loss in few neurons, while the high doses potentiated reactive astrogliosis and neuronal damage in the form large vacuolation of neuropil around damaged neurons (Mitra et al. 2013). To reverse the neuropathological outcomes, scientists have suggested using an anti-inflammatory agent for lightening the inflammatory signs and ameliorating its outcomes. Although the anti-inflammatory agent aided in inflammation retraction, it could not reverse the imbalance of the ROS (Kara et al. 2015; Frances et al. 2016). Further investigation advised using a multi-factorial agent as estradiol, the predominant estrogen, as a convenient candidate for the treatment of SCI. The potential effects of estradiol are attributed to the attenuation of neuropathological damage within the tissue by reduction of intracellular Ca2+ amplification, inflammatory cells infiltration, and ROS generation that was correlated with apoptotic pathways. In addition to the associated correlation between estrogen and endothelial cells acceleration for recovery in injured areas (Losordo and Isner 2001), estradiol has also been used as a brain-derived neuroprotective factor against neurodegenerative diseases models as cerebellar ataxia (Leranth et al. 2000; Sierra et al. 2003; Sribnick et al. 2003; Angeles et al. 2015). The plasticity of estrogen in neurological damage outcome was clearly depicted in female subjects in contrary to male ones as shown by Kupina et al. (2003) and Bayir et al. (2004) who demonstrated the limited neuroprotective effect evolves in male than females as the observable cytoskeletal protein degradation, and the cell membrane dysfunction occurs early in males following experimental traumatic brain injury. This could be explained by the differential quantification of estrogen between male and female, as in the latter, it is considered as an essential sex hormone produced by ovaries in large quantities, while in the male, it is produced in tiny quantities by testis. A study by Samantaray et al. (2010) confirmed that the administration of estradiol following SCI prevented the microgliosis and astrocytosis and reduced the apoptotic changes, as well as it aided in the promotion of angiogenesis and the growth of microvessel that protected cells from ischemia caused by blood vessels interruption in response to the injury. The estrogen produces its genomic and non-genomic action through the presence of their ubiquitous estrogen receptors (ERs), ER-α and ER-β that are widely expressed in the multiple brain regions including the cerebellum (Kuiper et al. 1998; Hazell et al. 2009). The co-localization of these estrogen receptors was observed in whole cells of the cerebellar trilaminar architecture during ontogeny and also in adulthood stages (Jakab et al. 2001; Perez et al. 2003). The necessity of estrogen receptor-β for neuronal endurance and glial proliferation during neurodegenerative disorders has been shown as it was highly expressed in neuron and glial cells (Yang et al. 2001). The aim of this study was therefore to use the cerebellar layers in particular to assess the effect of Kainic acid in inducing SCI. A further aim of the study was to evaluate the usage of estradiol to amend the histoarchitecture lesions of the cerebellum. To assess the effect of both Kainic acid and estradiol, a multiple indicator approach such as the use of genetic profiling of apoptotic, microgliosis, and inflammatory markers was used. In addition to this approach, the histological evaluation, the glial fibrillary acidic protein (GFAP) marker alongside the principal

intermediate filament protein of mature astrocytes was used to measure the mean density of astrogliosis in both the SCI group and estradiol-treated group by immunohistochemical and gene expression profiling analysis.

Material and methods

Experimental design

This experiment was carried out on 45 adult male Westar rats weighing about 250 g body weight. To ensure that the environment will have the same effects on the subjects' appetite and behavior, animals were housed individually in separate cages and had a free access to food and water for 7 days prior to the initiation of the experiment. The study was conducted according to the guidelines of the National Research Center Ethical Committee, Egypt; registration number (09/189) and followed the recommendations of the National Institute of Health for the care and use of laboratory animals. Animals were assigned to one of the following four groups: SCI group ($n = 13$), estradiol-treated group ($n = 13$), control group ($n = 6$), and a sham control group ($n = 13$). No manipulations were conducted on the control group, while the sham group was subjected to identical surgical procedures in exactly the same way as the treated group with the exception that this group was injected with an equal amount of cerebrospinal fluid (CSF) instead of Kainic acid glutamate excitotoxic substance.

SCI induction and treatment operation

The anesthetization process was performed using intraperitoneal administration of ketamine-xylazine combination. During surgery, a thermostatically regulated heating pad was used to maintain the body temperature of the subject animal. Under the guidelines of Braga-Silva et al. (2007), an incision was made between T-13 and L3 to expose the injection area. To reach the exact destination and also to avoid central canal damage, stereotaxically toxin KA (1.5 μl of 2.5 mM) were bilaterally injected through a 10-μl Hamilton syringe attached to a Microdrive pump. The estrogen administration (4 mg/kg) step was fulfilled 20 min after KA administration and was then followed by a daily injection (2 mg/kg) for five constitutive days.

Sample collection and staining

The cerebellum specimens were obtained from the euthanized animals after 24 and 72 h of the first dose and then at 7, 14, and 30 days. The samples were placed into 10% neutral-buffered formaldehyde for 24 h and were then impregnated and embedded in paraffin and sectioned. Following the sectioning, a deparaffinization in xylene and hydration using a descending grade of alcohols was made; the samples were stained with different types of stains in consonance with Carson (1990) protocols and were examined by Olympus CX41 microscope attached to an Olympus C-7070 digital camera. In addition to the routine staining with H&E, the phosphotungstic acid hematoxylin stain was used to distinguish the glial fibers according to the following steps: The sections were mordanted in Zenker's solution overnight at room temperature; this was followed by washing in running tap water for 15 min; and the sections were then placed in Logul's iodine solution for 15 min. The sections were decolorized using 95% alcohol for 1 h, were rinsed three times in distilled water, and were placed in 1% potassium permanganate for 5 min. The sections were washed in running tap water for 10 min and were decolorized again in 5% oxalic acid for 5 min. Finally, the sections were merged in the phosphotungstic acid-hematoxylin solution overnight at room temperature. The cresyl violet stain was used to highlight the Nissl granules by a blue-purple color through dipping a serial section of 5 μm in a working cresyl violet solution with few drops of acetic acid for 10 min. The toluidine blue stain was used to accentuate the cytoarchitecture of the cerebellar layers by transferring the slides into a toluidine blue solution for 10 min. Immunohistochemical staining was applied on paraffinized sections to visualize the increase and decrease of astrogliosis resulted from injury using an anti-GFAP marker that bound to Astrocytes' glial fiber acidic protein. For preserving the tissue sections well adhered to the glass, a positively charged coated slides were used on IHC staining. The protocol was applied according to Abcam guidelines (www.abcam.com/technical.IHC-P) as following: The sections were deparaffinized and rehydrated using standard methods and then were immersed in a pretreated heat-induced epitope antigen retrieval solution buffer for 15 min in a scientific microwave (at 100 °C) followed by washing with phosphate buffer saline. The slides were incubated with Triton 100× (Sigma-Aldrich) blocking reagent and 5% normal goat serum for 1 h at room temperature and were then incubated for 24 h at 4 °C with anti-GFAP primary antibody (Sigma-Aldrich; USA; G3893; 1:300) in PBS with 5% normal goat serum and 1% fetal bovine serum (FBS; Sigma-Aldrich). After 24 h, the sections were incubated for 1 h at room temperature with the FITC-conjugated secondary antibody (goat anti-mouse, Sigma-Aldrich, USA, 1:200); then the slides were coverslipped with anti-fade Vectashield reagent (Life technologies; USA; P36931). The examination was conducted on a fluorescent microscope (OPTIKA, Italy) and photographed at ×40 magnification for analytical

assessment with the aid of OPTIKA VIEW imaging software under default settings. The statistical assessment for all morphological data was analyzed by ImageJ software (NIH, USA) and Microsoft Excel 2016 software (USA).

RT-PCR analysis

The cerebellum specimens were frozen at − 80 °C until use. These samples have undergone RNA extraction process using QIAamp RNeasy Mini kit (Qiagen, Germany, GmbH). It was accomplished by mixing 100 mg of the specimen with 600 μl RLT buffer including 0.6 μl of β-mercaptoethanol. The sample homogenization was performed using Qiagen tissueLyser. The total RNA purification was then followed by DNase digestion step for elimination of the remaining DNA. These primers (Metabion®, Germany) were employed in a 25-μl reaction that included 0.5 μl of each primer in addition to 12.5 μl of the 2× QuantiTect SYBR Green PCR Master Mix (Qiagen, Germany, GmbH), and with the aid of 0.25 μl of Reverse Transcriptase from Thermo Fisher, and a mix of 3 μl of RNA template to 8.25 μl of water. The primer sequences, target genes, amplicon sizes, and cycling conditions for SYBR green RT-PCR are illustrated in Table 1. The variance of gene expression between samples was determined by comparing the sham CT values with the positive control under the guiding of "ΔΔCt" method as stated by Yuan et al. (2006). This operation was fulfilled by Stratagene MX3005P RT-PCR Machine.

Results

Since the main objective of this study was to determine the neuroprotective effect of estradiol on injured cerebellum in response to SCI, the confirmation of KA neurodegeneration in cerebellar layers was addressed by histological, and immunohistochemical visualization. During the brain autopsy, the gross anatomical inspection of the cerebellum did not show any evidence of cavitation or vacuolization. It only demonstrated the presence of severely congested blood vessels in dorsal and ventral surfaces (Fig. 1a). Although during the 24 h post-KA administration, the routine histological examination showed an ordinary folia pattern, the preliminary signs of neurodegeneration throughout the cerebellar cortical layers, congested blood capillaries, and activated microglial response were noticed. These signs were more obvious in the Purkinje cells layer in comparison to other sub-layers (Fig. 1b). The 72-h audit following injury revealed that the Purkinje cells layer faced an intense morphological alteration in its organization and was therefore displayed as an extensive and segmental Purkinje cell depletion. Some cells were observed within a vacuolated neuropil as hypereosinphilic shrunken perikaryon with pyknotic nuclei and attenuated dendritic arborization (Fig. 1c, d).

The inspection at 7 days after the induction of SCI revealed a disruption of neuronal arrangement, and a massive cytotoxic edema in addition to faint or loss of Nissl granules staining that was accompanied by nuclear envelope disassembles,

Table 1 Primers sequences, target genes, amplicon sizes and cycling conditions for SYBR green RT-PCR

Target gene	Primers sequences	Reverse transcription	Primary denaturation	Amplification (40 cycles)			Dissociation curve (1 cycle)		
				Secondary denaturation	Annealing (optics on)	Extension	Secondary denaturation	Annealing	Final denaturation
Rat β-actin (Banni et al. 2010)	TCCTCCTGAGCGCA AGTACTCT GCTCAGTAACAGTC CGCCTAGAA	50 °C 30 min	94 °C 5 min	94 °C 15 s	60 °C 30 s	72 °C 30 s	94 °C 1 min	60 °C 1 min	94 °C 1 min
Caspase 3 (Shi et al. 2009)	AGTTGGACCCACCT TGTGAG AGTCTGCAGCTCCT CCACAT				53 °C 30 s			53 °C 1 min	
GFAP (Liu et al. 2012)	CCTTGAGTCCTTGC GCGGCA TTGGCCCTCCTCCT CCAGCC				55 °C 30 s			55 °C 1 min	
Iba1 (Le Coz et al. 2014)	TCC CAT CCA ACC TCT CTT CC GCA GCC TCA TCG TCA TCT C				61 °C 30 s			61 °C 1 min	
IL1B (Wang et al. 1997)	CTCTGTGACTCGTG GGATGATGAC TCTTCTTCTTTGGG TATTGTTTGG				60 °C 30 s			60 °C 1 min	

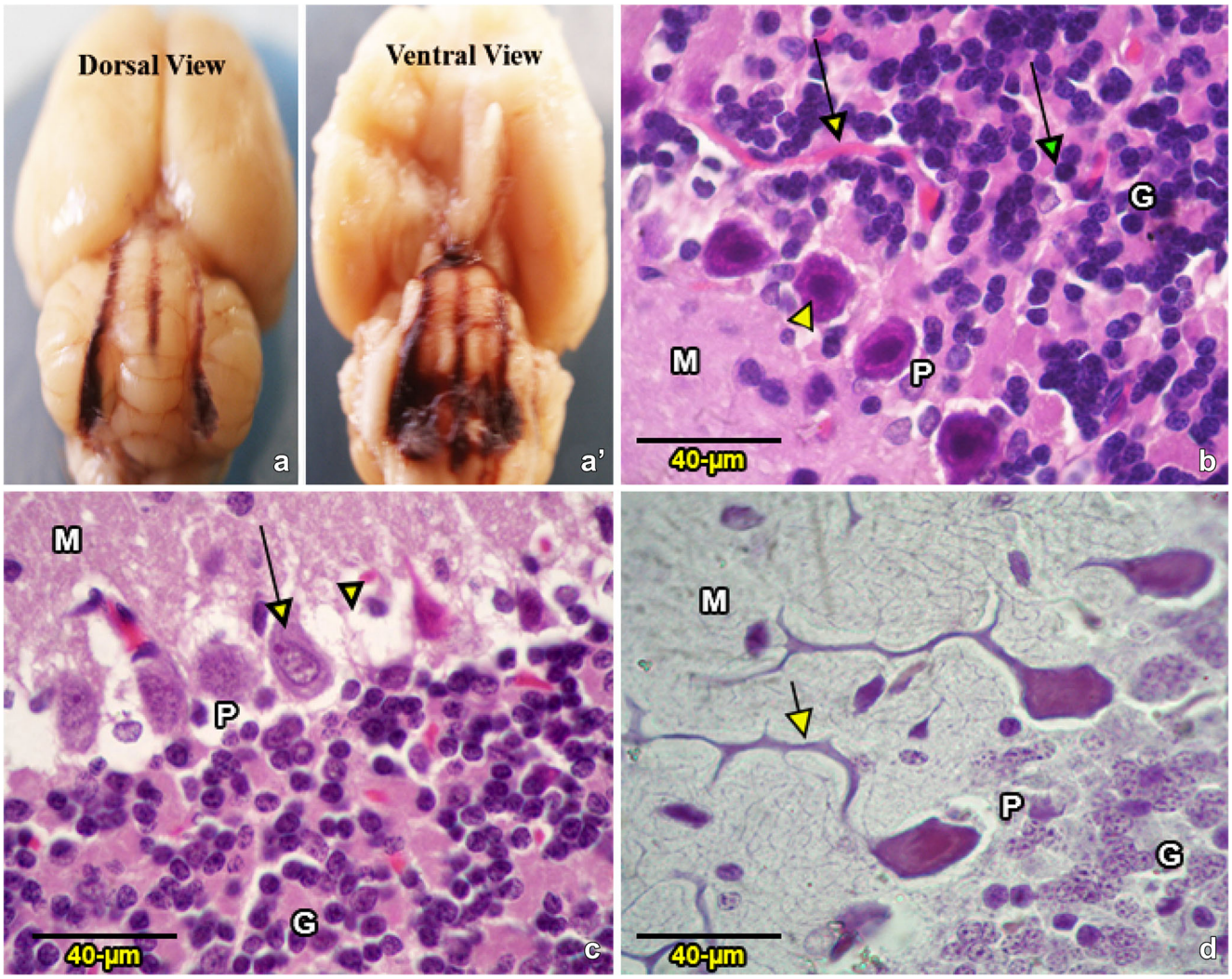

Fig. 1 Inspection 24 h following injury is showing. **a**, **a′** Both dorsal and ventral surfaces are presenting conspicuous congestion on blood vessels during gross inspection. **b** (H&E) The three layers of cerebellar cortex; the granular layer (G), Purkinje layer (P), and the molecular layer (M) showed engorged blood capillaries (yellow arrow), in addition to the neurodegenerative changes represented by shrunken neuronal soma with dark eosinophilic cytoplasm of Purkinje neurons (arrow head) and pyknotic nuclei of granular neurons (green arrow). **c** (H&E) At 72 h scanning; obvious alteration of Purkinje cells architecture with loss in nuclear morphological details and loss of their nucleoli (arrow), others were located within a vacuolated neuropil (arrow head). **d** (PTAH) attenuated dendritic arborization of Purkinje cell are noticed (arrow)

central chromatolysis, and spewing of nucleolus. Finally, this cell lysis appears as ghost that elicited an immune response identified as gliosis (Fig. 2a). The granular layer appeared relatively preserved in comparison to other cerebellar layers; nevertheless, pyknotic nuclei, raised gliosis, and congested blood capillaries were detected in the sections (Fig. 2b). These reactive changes in glial cells did not spare the molecular layer as they were emphasized by IHC inconstant positive immunoreactivity to gliosis alongside collateral damage in white matter that was presented as occasional vacuolation (Fig. 2c–e).

From the 14th-day to the 30th-day assessment, most of the neurons degenerated areas revealed a high percentage of proliferated hypertrophied astrocytes nearby neuronal loss of both Purkinje and granular layers (Fig. 3a, b). The fluorescence imaging in low magnification presented a clearly distinct cerebellar cortical layers where the Purkinje layer clearly stood out between the granular and the molecular layers. The conspicuous emergence of a positive reaction on large pyriform neurons in one cell thick row alignment made the identification of the Purkinje layer undoubtedly (Fig. 3c). The astrogliosis was also confirmed by IHC assessment that was markedly increased in the mean density of GFAP-positive astrocytes of the granular layer from control's moderate distribution to lesion's intense distribution (Fig. 3d, e).

Stereotaxic injection of CSF into the spinal cord of sham control group neither produced noticeable neuronal degenerations nor necrotic signs in the cerebellar sub-layers in comparison to the SCI group (Fig. 4a, a′, b).

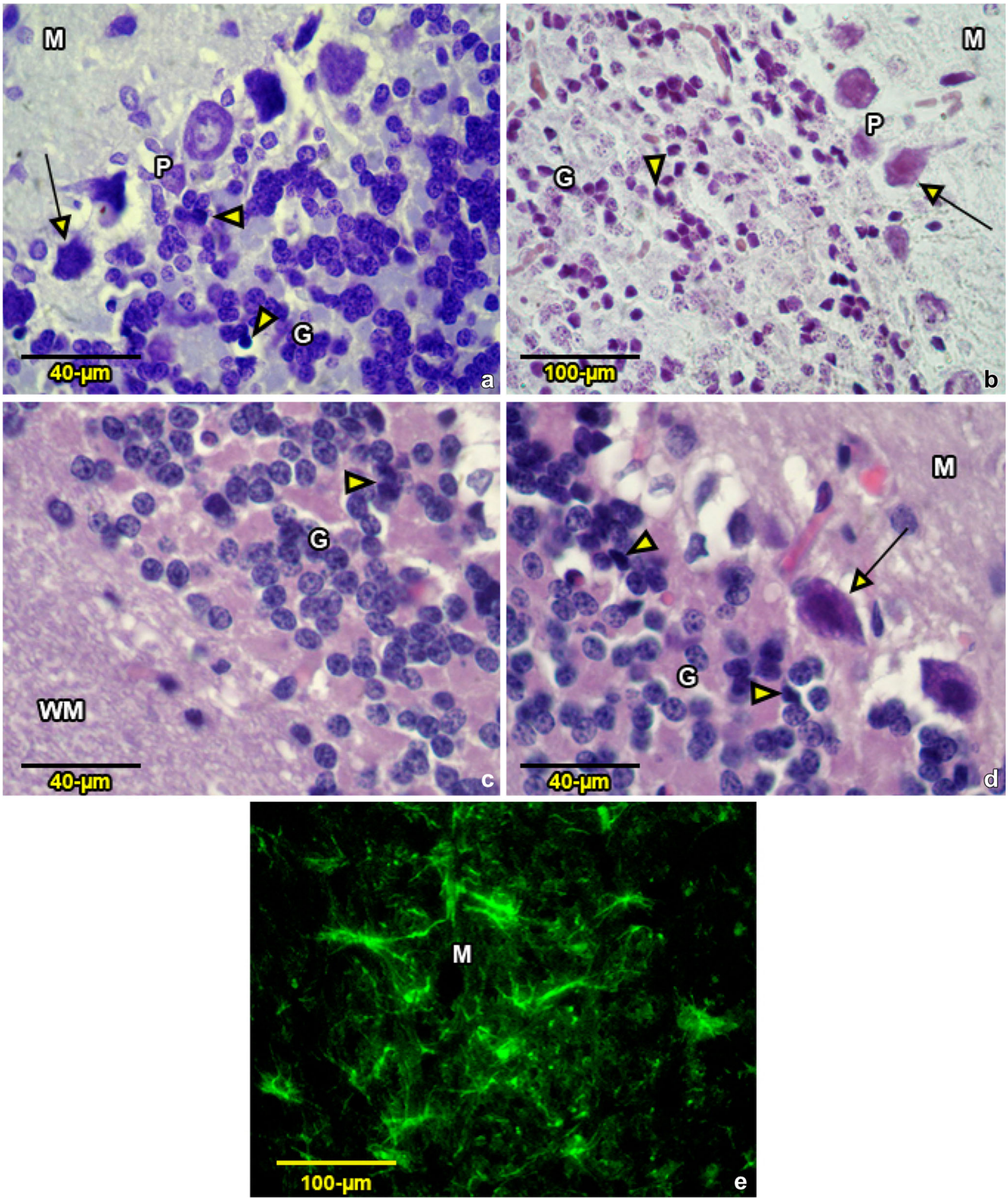

Fig. 2 Observations at the seventh day scanning in SCI specimens. **a** Cresyl violet. **b** PTAH. **c**, **d** H&E showed variable stages of Purkinje cell lysis (arrow), pyknosis of the granular cell neurons (arrow head), beside the election of immune-response in all sub-layers that was observed by an increase the immunoreactive GFAP cells in the molecular layer (M). **e** GFAP IHC

The histopathological inspection of the cerebellum in estradiol-treated group indicated that most of the neurodegenerative changes observed previously gradually diminished, while the laminar architecture became highly

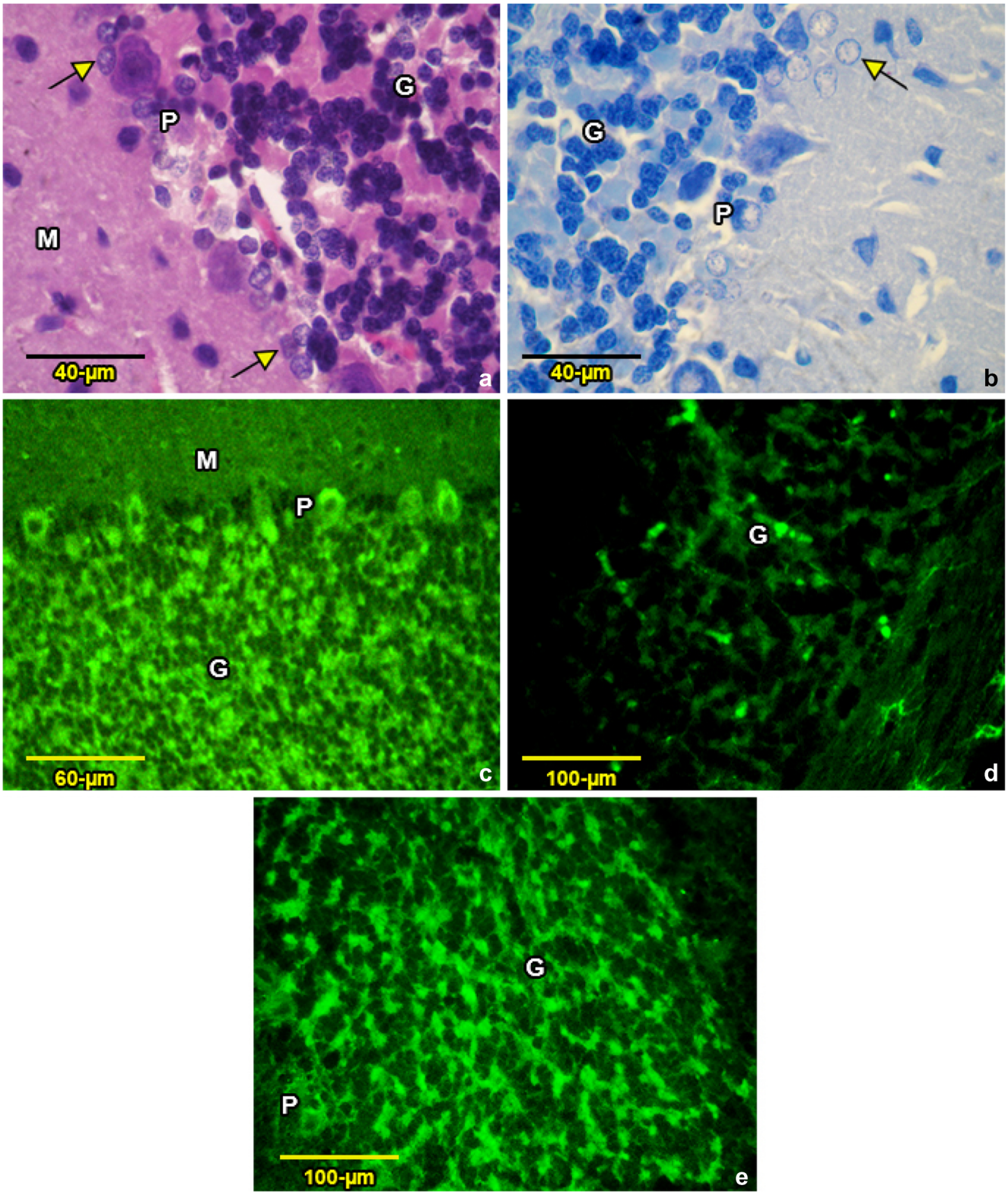

Fig. 3 Observations at the 14th day following injury. **a** H&E and **b** toluidine blue showed an increase of hypertrophied astrocytes (arrow) in all layers. **c** GFAP IHC confirmed a clearly distinct three cerebellar layers; the granular layer (G), Purkinje layer (P), and molecular layer (M). **e** GFAP IHC, an observable increment in the mean density of GFAP positive astrocytes in the granular layer (G) as well as reacted Purkinje cells (P) in comparison to the control group (G). **d** GFAP IHC

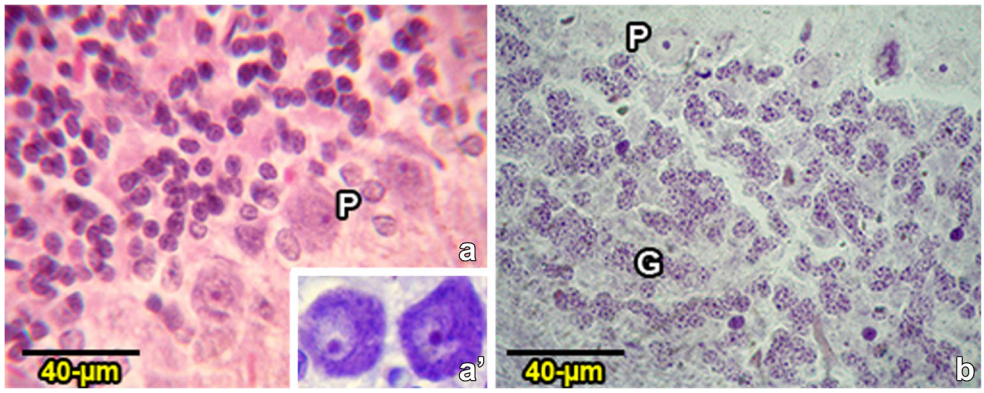

Fig. 4 The sham control group did not show any noticeable variation compared to the control group, whereas healthy Purkinje neurons (P) with a central spherical nucleus and prominent nucleoli were dominant in the Purkinje layer (**a** H&E; inset a′, cresyl violet), while the granular layer appeared crowded with fine granular nuclei (G) confirming unharmed tissue (**b** PTAH)

organized and began to be more evident, especially Purkinje cell layer which was the most predominant layer (Fig. 5a, b). These variations depended on the time of exposure to the neuroprotective estrogen, where at the 24 h to 1 week of the first dose, the microscopical examination did not show significant differences in comparison to SCI specimens as it included indistinct boundaries of Purkinje cells, densely stained scanty cytoplasm, and nucleus with interruption of dendritic arborization (Fig. 5c, d).

An optimistic improvement became more obvious at 14th until the 30th day, as the Purkinje cell population was widely distributed along the entire length of the Purkinje cell layer, and also the granular neurons with finely dispersed chromatin were identified, although few degenerated Purkinje and granule neurons with prominent nuclei of astrocyte invasion were still prevalent (Fig. 6a–c). The IHC inspection highlighted a mild distribution of strong immunoreactivity star cell astrocytes with their branching processes in the cerebellar layer that confirmed the amelioration process to SCI sections (Fig. 6d).

Statistical analysis

In order to determine the modulation degree of gene expression in the cerebellar specimens following induced SCI, and the protective events that were endorsed by the administration

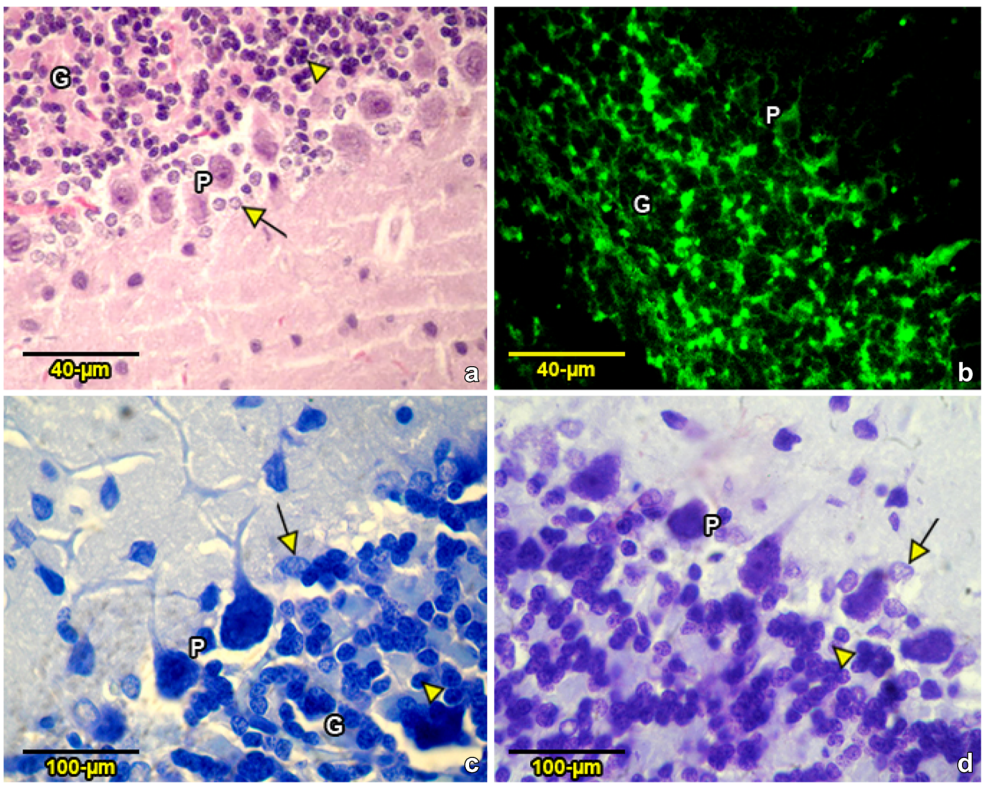

Fig. 5 The estradiol-treated group at the seventh day inspections presented a gradually diminished degenerative changes with a decrease in the number of shrunken, pyknotic nuclei of Purkinje cell (P) and granular cells (arrow head) and a decrease in the number of large pale astrocytes (arrow) beside the signs of organization in the laminar architecture. **a** H&E. **c** Toluidine blue. **d** Cresyl violet. **b** GFAP IHC. An observable increment in the mean density of GFAP positive astrocytes in the granular layer (G) as well as reacted Purkinje cells (P)

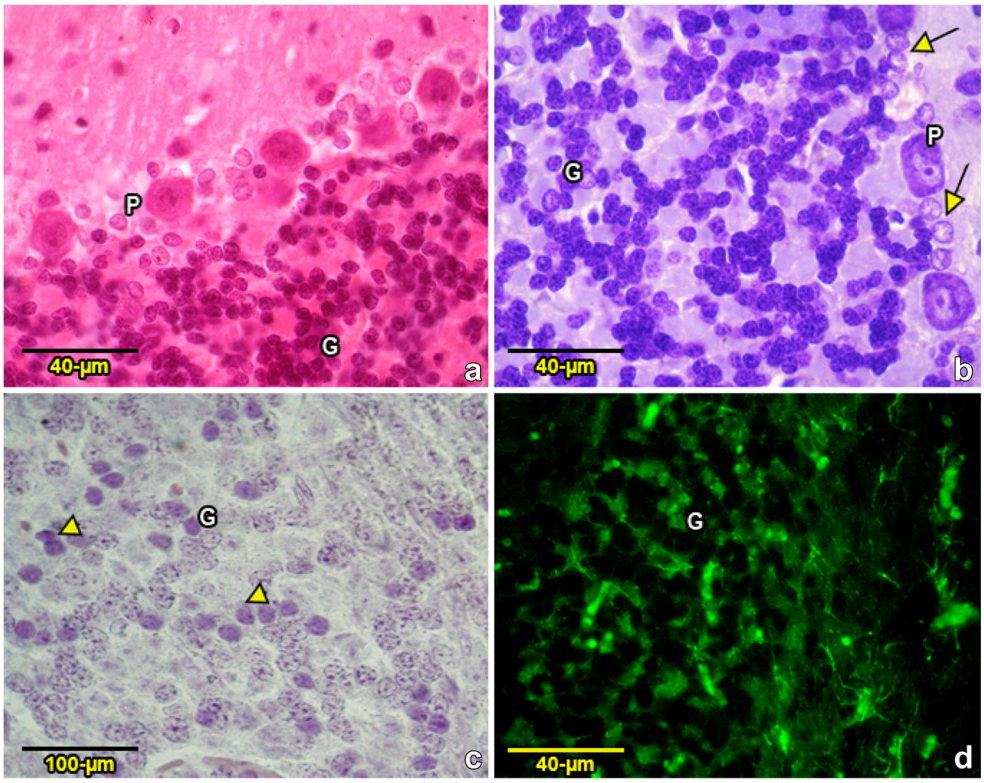

Fig. 6 Estradiol-treated group at the end of the trial, the Purkinje cell layer appeared crowded with normal phenotype of Purkinje cells (P) (**a** H&E), moderate astrocytic infiltration with signs of vanishing (arrow) (**b** cresyl violet), the granular layer presented a decline in the pyknotic neuronal percentage (arrowhead) (**c** PTAH), a remarkable reduction in positive immunoreactivity to GFAP (**d** GFAP IHC)

of estrogen, cerebellar samples were introduced to qPCR amplification process for the following genes: the apoptotic caspase-3, IL-1β, Iba-1, and GFAP (Table 1). At first 24 h following KA injection, the caspase-3 gene expression was significantly upregulated ($P < 0.05$) in comparison to the control group and was then followed by a gradual increase in expression until second-week, and then a non-significant decrease ($P > 0.05$) at the fourth week, although there was still a highly significant expression ($P < 0.001$) when compared to the control group at the end of the trial. The estradiol-treated group presented, at first day, a highly significant increase ($P < 0.001$) in comparison to the control group, taking into consideration that there was no significant difference between SCI and estradiol groups ($P > 0.05$). There was, however, a gradual decrease until the end of trial; therefore, there was a significant difference ($P < 0.05$) between the estradiol and SCI groups as depicted in Fig. 7a. The astrocytic proliferative gene from the first day of lesion induction until the end of the trial showed a gradual but significant increase ($P < 0.05$) in its expression in comparison to the control group, while the estradiol group presented a highly significant increase ($P < 0.001$) in its expression at the first day when compared to the control group and a highly significant difference ($P < 0.001$) when compared to the SCI group at analogs period. This expression displayed a gradual significant decrease ($P < 0.05$) until the end of the trial, although there was still a significant expression ($P < 0.05$) in comparison to the control group as shown in Fig. 7b. The microglial activation expression gene at first day of exposure to KA excitotoxicity exhibited a highly significant increase ($P < 0.001$) in its expression when compared to the control group and then was followed by a slight increase during the following days that faced a sudden and non-significant decrease ($P > 0.05$) at the second week until the end. This reduction did not approach the normal level, showing a highly significant ($P < 0.001$) difference between its expression and the control group. Although the Iba-1 gene showed a significant reduction ($P < 0.05$) in its expression at first day of the treatment, a profound highly significant variation ($P < 0.001$) persisted in comparison to the control level. This expression has undergone gigantic decline through trial's time-window, whereas, at the end of the experiment, it displayed a non-significant difference ($P > 0.001$) in comparison to the control group approaching the normal level and drifting away from the treated group expression showing a highly significant difference ($P < 0.001$) as described in Fig. 7c. The IL1B gene profiling presented a significant alteration in its expression in response to both lesion induction and treatment operations, whereas at first day, it was upregulated significantly ($P < 0.05$) and highly significantly ($P < 0.001$) in SCI, and estradiol specimens, respectively, although there was a significant difference ($P < 0.001$) between SCI and estradiol groups. From this point until the end of the experiment, a conspicuous repulsion in the trajectory of both expressions was noticed, whereas the SCI group expressed a highly significant increase ($P < 0.001$), while the estradiol group expressed a highly significant decrease in the IL1B gene

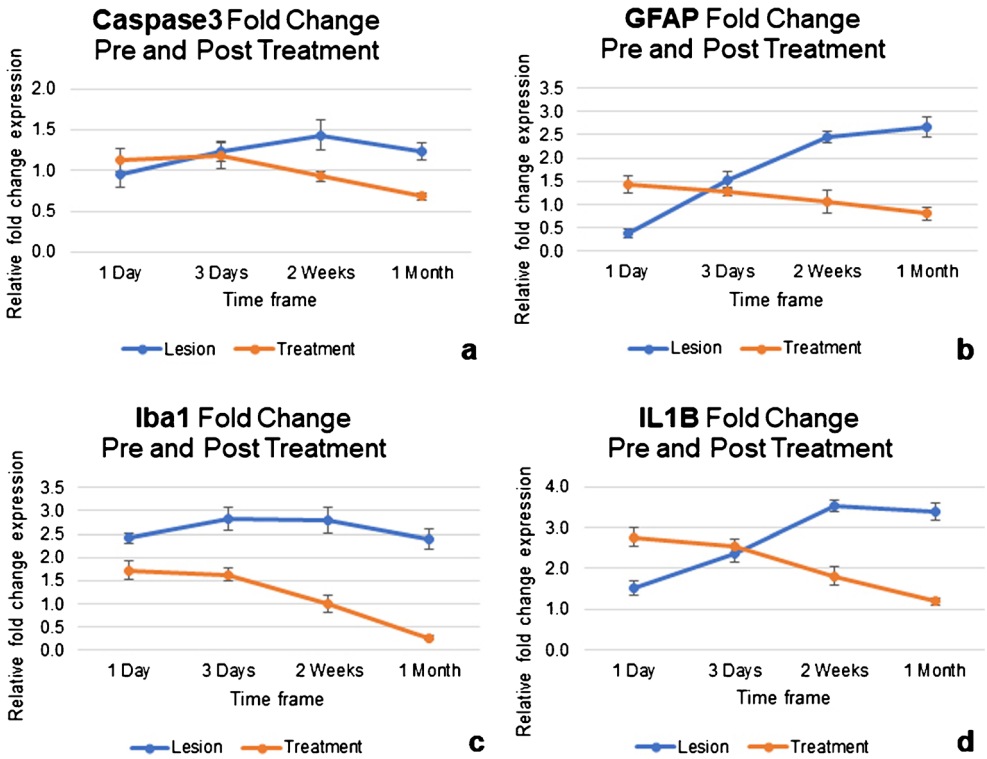

Fig. 7 Chart depicting the genetic expression profiling of SCI and estradiol-treated groups. **a** Caspase-3. **b** GFAP. **c** Iba-1. **d** IL1β

expression. Although both trajectories did not approach the normal level, there was a highly significant difference ($P < 0.001$) between the SCI and estradiol group at the end of the first month (Fig. 7d). The fold changes of each gene expression during the experimental period are depicted in Table 2.

To estimate the extent of neurodegenerative actions of KA and the protective role of estradiol on the cerebellar layer, light microscopical analysis of HE and PTAH stained sections was examined at ×100 magnification to compute the number of apoptotic and degenerated cells of granular and Purkinje layers in addition to the astrocytic propagation density. Cells displayed morphological changes away from famed (unambiguous) neuronal morphology, as cell shrinkage with dense cytoplasm and nuclear pyknosis with irregularly shaped nuclei and non-detectable nucleoli were counted in the cortical cerebellar layers of the four experimental groups. A single-factor ANOVA was used to evaluate differences between the groups. The density of astrocytic propagations was confirmed in immunohistochemically stained sections where the GFAP positive immunoreactive astrocytes were counted. Fluorescent microscopy analysis of GFAP-stained sections of control group showed a few scattered immunoreactive astrocytes in all cerebellar sub-fields, while many reacted astrocytes were evident in the granular and Purkinje layers in GFAP-stained sections of treated group which is considered an indicator of a significant increase ($P < 0.05$) in astrocytic mean density whereas a + 2.47-fold increase in comparison to the control group was noted. Although the GFAP expression in estradiol groups showed a slight + 0.7-fold increase when compared to the control group, it showed a significant decrease ($P < 0.05$) when compared to the SCI group where the GFAP fold change in estradiol groups was retracted to − 0.5 of those of the SCI groups. This peak of increment in GFAP expression was

Table 2 Gene expression average fold changes with standard deviation during the experimental time period

Gene	Day	SCI	Estradiol
GFAP	1 day	0.38 ± 0.08	1.43 ± 0.19
	3 days	1.53 ± 0.18	1.27 ± 0.08
	2 weeks	2.46 ± 0.12	1.05 ± 0.25
	1 month	2.67 ± 0.22	0.81 ± 0.14
Iba1	1 day	2.41 ± 0.11	1.72 ± 0.2
	3 days	2.83 ± 0.24	1.64 ± 0.13
	2 weeks	2.79 ± 0.27	1 ± 0.19
	1 month	2.4 ± 0.21	0.27 ± 0.05
Caspase 3	1 day	0.96 ± 0.16	1.13 ± 0.14
	3 days	1.24 ± 0.12	1.18 ± 0.15
	2 weeks	1.43 ± 0.19	0.93 ± 0.06
	1 month	1.24 ± 0.1	0.68 ± 0.04
IL1B	1 day	1.52 ± 0.19	2.77 ± 0.22
	3 days	2.36 ± 0.19	2.53 ± 0.2
	2 weeks	3.53 ± 0.14	1.82 ± 0.22
	1 month	3.39 ± 0.21	1.2 ± 0.09

paralleled by the condensation of astrocytosis in HE-stained sections. The number of astrocytic infiltrations increased dramatically after KA intoxication (0.9-fold) ($P < 0.05$) in comparison to the control group, whereas the estradiol group showed a decrease (− 0.25-fold) in comparison to the SCI group. At the end of the experiment, a slight increase (0.4-fold) was counted in the estradiol group in comparison to the control group. To assess the apoptotic neurons of the granular layer, the quantitative analysis showed a significant increase ($P < 0.05$) in the fold change (5.15-fold) of the SCI group that was distinguished when equated to the control one, while the estradiol group showed only a 1.2-fold increase when also equated to the control group and a − 0.6 decrease when compared to the SCI group. Incompatible with the aforementioned results, the SCI group presented a significant increase ($P < 0.05$) in the fold change of degenerated Purkinje cells where it reached about 9-fold of those of the control one. Nevertheless, this fold decreased by − 0.5 following the estradiol treatment, and therefore, the estradiol group exhibited only a 4-fold of the control group. These statistical results are depicted in Table 3 and Fig. 8.

Discussion

While examining the spinal cord tissue structure upon injury, variable degrees of neuronal and cellular degenerations were found that were accompanied by an increase in inflammation cascade initiation in the entire tissue architecture. These neuronal changes have been distinguished crawling into spinocerebellar tract reaching the cerebellar layers and prompting major alteration in its cellular composition. These observations have been noted by many investigators (Gulgun et al. 2015; Nishant and Joe 2016). From this point and depending on the observation that spotted a huge influence on body behavioral functions, the cerebellum was selected as a target object for treatment in the current study. One of the most strategies that was used to mimic the histoarchitecture alteration upon SCI was the induced neurotoxic lesioning by glutamate receptor agonist technique that had the ability to produce a chain of neurodegenerative changes which finally led to neuronal components loss. In order to achieve this neuroprogressive effect and in line with previous study of Yezierski et al. (1993), the selected KA dose (1.5 μl of 2.5 mM KA) had resolute almost the aftermost effect to traumatic induced injury that could be interpreted by the potent induced neuronal apoptosis through activation of an excitatory neurotransmitter glutamate receptors within spinal cord tissue (Drexel et al. 2012; Lai et al. 2014) in addition to initiation of caspase-3 pathways that caused a disturbance of ca+2 influx leading to intra-cellular overload and finally mitochondrial dysfunction (Wang et al. 2005). Based on the histopathological inspection of the sham control group, the doubt that injury could have resulted from needle invagination inside the tissues was eliminated. Furthermore, it assured that the surrounding environment did not have a stress impact on trial specimens' health status. Through interference with many of intracellular destructive cascades as free radical production, a decline of gliosis reaction, and endorsement of angiogenesis, estrogen (estradiol), was considered one of the potent neuroprotective substance that has diversified anti-oxidant, anti-inflammatory, and anti-apoptotic functions (Siriphorn et al. 2012; Samantaray et al. 2016). Exogenous estrogen was used to inspect its capability as a promising neuroprotective therapy to the cerebellum of a chemically induced SCI. The purpose behind selecting male subjects instead of a female was to eradicate the notion noted by Sua'rez et al. (1992) of the influence of endogenous female sex hormone on inducing GFAP expression. The gross inspection following the injury process showed no evidence of shape abnormalities except the existence of a severe congestion on both surfaces which was a reflection of clogged blood capillaries. Even though we did not stain a specific marker for Purkinje cells identification, they expressed a positive immunoreactivity which was owned

Table 3 Neurodegenerative signs average fold changes between experimental groups

	Average			Control & SCI		SCI & Estradiol		Control & Estradiol	
	Control	SCI	Estradiol	Fold change	P- Value significance	Fold change	P- Value significance	Fold change	P- Value significance
Pyknosis on granular layer	4±1	24.6±3.4	8.8±2.2	Lesion ↑ 5.15	0.00000107<0.05 Significant	Treated ↓ -0.6	0.00002127<0.05 Significant	Treated ↑ 1.2	0.00201374<0.05 Significant
Astrocytic infiltration	8.8±1.9	16.8±3	12.6±1.7	Lesion ↑ 0.9	0.00107870<0.05 Significant	Treated ↓ -0.25	0.02661322<0.05 Significant	Treated ↑ 0.4	0.01034093<0.05 Significant
Degenerated Purkinje cells	0.4±0.5	4±1.6	2±0.7	Lesion ↑ 9	0.00133713<0.05 Significant	Treated ↓ -0.5	0.03251559<0.05 Significant	Treated ↑ 4	0.00394977<0.05 Significant
GFAP positive cells	17±2.2	59±11	29±2.4	Lesion ↑ 2.47	0.00003204<0.05 Significant	Treated ↓ -0.5	0.00034549<0.05 Significant	Treated ↑ 0.7	0.00004027<0.05 Significant

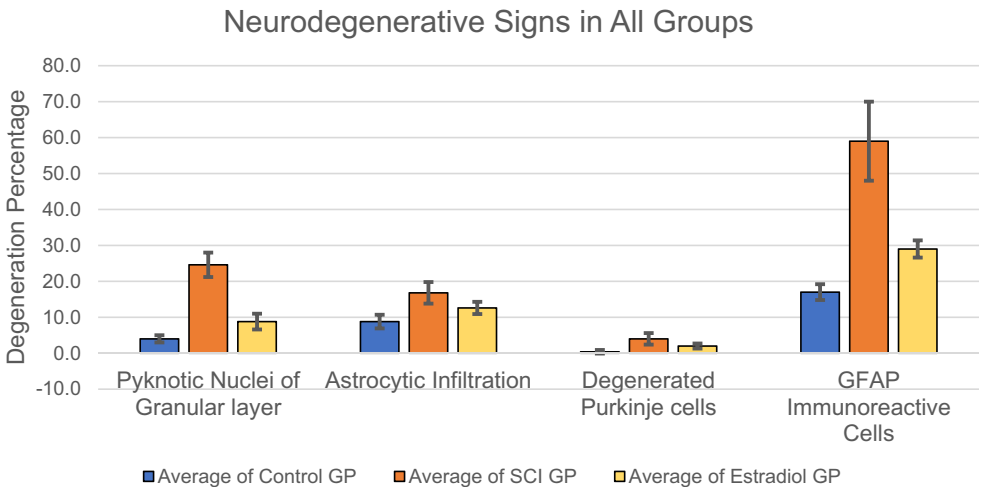

Fig. 8 Chart of the average various neurodegenerative signs between the control under the influence of KA, estrogen treatment

to the precise warping of Bergman astroglia's dendrites around the Purkinje's dendritic spines and its excitatory synapses. This result agrees with those obtained by Lordkipanidze and Dunaevsky (2005) who confirmed that Purkinje cells did not display a normal architecture in GFAP knockout mice. The Neuroinflammation and the subsequent increase in glial cell activation within a vacuolated neuropil were evident in the molecular layer, and this finding is also in an agreement with that presented by Wang et al. (2005) and Chen et al. (2005). Nevertheless, this astrocytosis and gliosis in the current experiment were more predominant in the Purkinje and granular cell layers. The severity of lesion in Purkinje layer could be explained by the unique circuitry of the cerebellum where the inhibitory glutamatergic Purkinje cells are the only cells in contrary to others that are receiving afferent from an excitatory parallel fiber of granule cells to reach its distal dendritic arborization into the outer synaptic molecular layer, while the intensity of injury on the granular layer is due to its gating role in inhibiting the signal flow into the cerebellum (Laurens et al. 2016). Additionally, during granular layer observation, the cerebellar granule cells (CGCs) showed a significant increase in apoptotic quantification and this could be explained by their particular vulnerability to excitotoxins of glutamate that is released by the motivation of kainite receptors (Verdaguer et al. 2002). The profiling of caspase-3 gene, the evidence to the apoptosis, through the experimental time-window showed a gradual increase in the treated group which supported the previous histopathological finding and interpreted the elevated apoptotic quantification, whereas it was activated following mitochondrial breakdown leading to apoptotic neuronal death (Lavrik et al. 2005). In the present investigation, the immunohistochemical localization produced a marked increment of astrocyte proliferation and hypertrophy that was also confirmed by the conspicuous up-regulation on expression of its gene, GFAP, which could be explained by the imminent interaction between the excessive inducing of glutamate by KA and the glutamate receptor activation on surface of these glial cells (Steinhäuser and Gallo 1996). As an extra-sign of this reactive gliosis, an obvious increase of microglia and subsequently in its cytokine release was distinguished by upregulation on the expression of their linked genes, Iba-1 and IL1-B, respectively. This gliosis played a certain interactive role by integrating neuronal inputs and modulating synaptic activity besides their partial role under a pathophysiological condition that endorses the secretion of a great number of cytokines, chemokines to act as pro-inflammatory or anti-inflammatory to perform a neurodestructive or neuroprotective function, respectively. The role of microglia to endorse or inhibit neuronal death relays on signals received from damaged neurons (Streit et al. 1999). The aforementioned results are in harmony with those obtained by Akbar et al. (2001) and Kato et al. (1999) who studied the effect of KA administration on different brain parts. On the other hand, the estrogen-treated group showed that an optimistic contra-finding in cerebellar laminated architecture was indicated by the identification of finely dispersed chromatin nuclei of granular neurons as well as by the wide distribution of Purkinje cells population along the entire length of Purkinje layer that could be explained under the notion of Spence et al. (2009) who confirmed the presence of the estrogen receptors on cerebellar Purkinje cells. This rejuvenation processes could be interpreted by estradiol intervention that in which its responsibility during the development of the cerebellar circuits in growing fetuses was indicated as it endorsed the development of dendrites, synapse formation, and spinogenesis throughout Purkinje and granular cells genesis (Garcia-Segura et al. 2001; Haraguchi et al. 2012). The caspase-3 gene, in response to estrogen intervention, displayed a regular decrease in its expression along the experiment that indicated the retraction of mitochondrial lysis and mitigation of Kainic acid toxicity. In addition to the above-mentioned findings, small-dispersed new capillaries were resolved in all sublayer that we suggest that it has a fundamental role in inducing recovery process by providing an adequate blood supply. This

explanation is supported by Jesmin et al. (2010) who reported the estrogen vital role in the angiogenesis process. Away from the classical pathway of excitotoxicity that relies on ER stress for inducing neuronal death, the estrogen anti-apoptotic function relies on a unique pathway that inhibits calcium uptake for preventing mitochondrial damage which is supported by localization of both estrogen receptors (ERa and ERb) on the mitochondrial surface (Chen et al. 2004). Contrary to expectations, the GFAP gene expression was upregulated at the treatment initiation period, which was in harmony with the finding of Ritz and Hausmann (2008) who highlighted a brief neuroprotective time-frame of estrogen at first days of treatment through stimulating early cytokines release and astroglial reactivity. This sudden upregulation is owned to estrogen endorsement to function and expression of GLAST and GLT-1, the glutamate transporters in astrocytes (Lee et al. 2009; Lee et al. 2012). These receptors main functions are preserving the ideal levels of glutamate in synaptic clefts for avoiding excitotoxic neuronal damage, in which estrogen enhances these transporters for inducing neuroprotection. At the end of the trial, we suggested that the GFAP retracted its expression as a response to estrogen impeding to inflammatory cells from migration into the nearby tissue beside the declined levels of pro-inflammatory cytokines. The modulation of the inflammatory cascade is considered the strongest point of estrogen therapy which prevents the infiltration of microglial cells and subsequently its cytokine elaboration in the injured tissue (Sribnick et al. 2010). One of the main inflammatory mediators that are released from activated glial cells is interleukin-1 beta (IL-β) that its existence reflects the actual percentage of the inflammatory phase in the injured area. KA has induced the expression of IL-1 β as early as 24 h post-lesioning; this was due to its localized effect to IL-1 β receptors that was expressed in the soma of cerebellar Purkinje cells (Motoki et al. 2009). Our findings presented an optimistic improvement through the trial time-window in the expression level of IL-1β, where the estrogen, the IL-1β receptor antagonist, had a dosage and a zone-dependent influence on neuronal endurance following KA-induced neurodegeneration (Panegyres and Hughes 1998). This expression was in harmony with GFAP expression, indicating a true reduction in the inflammatory stage. Whereas the microgliosis is considered a decisive factor on the battle against the secondary insult of any degenerative changes in the brain, our finding presented a significant descending of Iba-1 gene expression. While at the end of the trial, the expression approached the normal level confirming the histological finding that showed a reduction in microglial quantification following the estrogen treatment intervention. This reduction could be contributed to the ability of estrogen to constrain microglial activation or to modulate the active once to their resting state (Paolicelli et al. 2011).

Conclusion

Although the cerebellar histoarchitecture at the end of the experiment did not fully recover and the consequences of KA intoxication was not entirely inverted, the estradiol-treated sections whether stained conventionally or immunohistochemically presented a major improvement in the cellular composition and tissue arrangement toward the normal architecture. It therefore appears that estrogen played an influential factor on ameliorating the inflammatory signs and attenuating the neuropathological impairment within the cerebellar layers; therefore, it could be used as a supportive agent for other medication since it is a natural endogenous hormone with no side effects within in the conservative ranges.

References

Akbar MT, Wells DJ, Latchman DS, de Belleroche J (2001) Heat shock protein 27 shows a distinctive widespread spatial and temporal pattern of induction in CNS glail and neuronal cells compared to heat shock protein 70 and caspase-3 following kainite administration. Brain Res Mol 93(2):148–163

Angeles MA, Iñigo A and Luis MG (2015) The neuroprotective actions of oestradiol and oestrogen receptors. Nature Reviews Neuroscience16: 17–29

Bruce AJ, Baudry M (1995) Oxygen free radicals in rat limbic structures after kainate-induced seizures. Free Radical Biology and Medicine 18(6):993–1002

Banni M, Messaoudi I, Said L, El Heni J, Kerkeni A, Said K (2010) Metallothionein gene expression in liver of rats exposed to cadmium and supplemented with zinc and selenium. Arch Environ Contam Toxicol 59:513–519

Bayir H, Marion DW, Puccio AM, Wisniewski SR, Janesko KL, Clark RS, Kochanek PM (2004) Marked gender effect on lipid peroxidationNafter severe traumatic brain injury in adult patients. J Neurotrauma 21:1–8

Braga-Silva J, Gehlen D, Roman JA, da Costa JC, Machado DC, Faúndez M, Orsi RB, Braga R (2007) Experimental model of spinal cord injury in rats with a device for local therapeutic agents access. Acta Ortop Bras 15(3):155–157

Carson FL (1990) Histotechnology. A self-instructional text, Connective and muscle tissue, Nerve, Phosphstungestic acid Hematoxylin. United State of America: American Society of Clinical Pathologists, PP. (163–164) (171–172) (176–177)

Chen Z, Duan RS, Quezada HC, Mix E, Adem A, Winblad B, Zhu J (2005) Increased microglial activation and astrogliosis after intranasal administration of kainic acid in C57BL/6 mice. J Neurobiol 62(2):207–218

Chen JQ, Delannoy M, Cooke C, Yager JD (2004) Mitochondrial localization of ERa and ERb in human MCF7 cells. Am J Phys 286: 1011–1022

Coyle JT, Puttfarcken P (1993) Oxidative stress, glutamate and neurodenerative disorders. Science 262(5134):689–695

Drexel M, Preidt AP, Sperk G (2012) Sequel of spontaneous seizures after kainic acid-induced status epilepticus and associated neuropathological changes in the subiculum and entorhinal cortex. Neuropharmacology 63:806–817

Frances C, Kimberley AM, Anna VL, Robert V (2016) Neurogenic inflammation after traumatic brain injury and its potentiation of classical inflammation. J Neuroinflammation 13:264

Garcia-Segura LM, Azcoitia I, DonCarlos LL (2001) Neuroprotection by estradiol. Prog Neurobiol 63:29–60

Gulgun S, Fu YH, Yu Y, George P (2015) Spinal cord projections to the cerebellum in the mouse. Brain Struct Funct 220:2997–3009

Haraguchi S, Hara S, Ubuka T, Mita M, Tsutsui K (2012) Possiblerole of pineal allo pregnanolone in Purkinje cell survival. Proc Natl Acad Sci U S A 109:21110–21115

Hazell GG, Yao ST, Roper JA, Prossnitz ER, O'Carroll AM, Lolait SJ (2009) Localisation of GPR30, a novel G protein-coupled oestrogen receptor, suggests multiple functions in rodent brain and peripheral tissues. J Endocrinol 202(2):223–236

Jakab RL, Wong JK, Belcher SM (2001) Estrogen receptor beta immunoreactivity in differentiating cells of the developing rat cerebellum. J Comp Neurol 430:396–409

Jesmin S, Mowa CN, Sultana SN, Shimojo N, Togashi H, Iwashima Y, Kato N, Sato A, Sakuma I, Hiroe M (2010) VEGF signaling is disrupted in the hearts of mice lacking estrogen receptor alpha. Eur J Pharmacol 641:168–178

Joshua JW, Marife A, Trace LS, Nicholas AG, Sabrina LL, Detlef HH, Roy VS (2014) Cerebellar zonal patterning relies on Purkinje cell neurotransmission. J Neurosci 34(24):8231–8245

Kara NC, Theodore LR, Dorian BMG (2015) Inflammation and neuroprotection in traumatic brain injury. JAMA Neurol 72(3):355–362

Kato K, Katoh-Semba R, Takeuchi IK, Ito H, Kamei K (1999) Responses of heat shock proteins hsp27, alphaB-crystalline, and hsp70 in rat brain after kainic acid-induced seizure activity. J Neurochem 73(1): 229–236

Kuiper GGJM, Shughrue PJ, Merchenthaler I, Gustafsson JA (1998) The estrogen receptor b subtype: a novel mediator of estrogen action in neuroendocrine systems. Front Neuroendocrinol 19:253–286

Kupina NC, Detloff MR, Bobrowski WF, Snyder BJ, Hall ED (2003) Cytoskeletal protein degradation and neurodegeneration evolves differently in males and females following experimental head injury. Exp Neurol 180:55–73

Lai TW, Zhang S, Wang YT (2014) Excitotoxicity and stroke: identifying novel targets for neuroprotection. Prog Neurobiol 115:157–188

Laurens W, Stephanie R, Pressler RT, Safiya IL, Wade GR (2016) Purkinje cell collaterals enable output signals from the cerebellar cortex to feed back to Purkinje cells and interneurons. Neuron 91(2):312–319

Lavrik IN, Golks A, Krammer PH (2005) Caspases: pharmacological manipulation of cell death. J Clin Invest 115:2665–2672

Le Coz GM, Fiatte C, Anton F, Hanesch U (2014) Differential neuropathic pain sensitivity and expression of spinal mediators in Lewis and Fischer 344 rats. BMC Neurosci 15:35

Lee ES, Sidoryk M, Jiang H, Yin Z, Aschner M (2009) Estrogen and tamoxifen reverse manganese-induced glutamate transporter impairment in astrocytes. J Neurochem 110:530–544

Lee E, Sidoryk-Wegrzynowicz M, Yin Z, Webb A, Son DS, Aschner M (2012) Transforming growth factor-alpha mediates estrogen-induced upregulation of glutamate transporter GLT-1 in rat primary astrocytes. Glia 60:1024–1036

Leranth C, Roth RH, Elswoth JD, Naftolin F, Horvath TL, Redmond DE (2000) Estrogen effects in substantia Nigra in primate. J Neurosci 20:8604–8609

Liu C, Li Y, Lein PJ, Ford BD (2012) Spatiotemporal patterns of GFAP upregulation in rat brain following acute intoxication with diisopropylfluorophosphate (DFP). Curr Neurobiol 3(2): 90–97

Lordkipanidze and Dunaevsky (2005) Purkinje cell dendrites grow in alignment with Bergmann glia. Glia 51(3):229–234

Losordo DW, Isner JM (2001) Estrogen and angiogenesis: a review. Arterioscler Thromb Vasc Biol 21(1):6–12

Mills CD, Xu GY, Johnson KM, Hulsebosch CE (2000) AIDA reduces glutamate release and attenuates mechanical allodynia after spinal cord injury. Neuroreport 11:3067–3070

Mitra NK, Goh TE, Bala Krishnan T, Nadarajah VD, Vasavaraj AK, Soga T (2013) Effect of intra-cisternal application of kainic acid on the spinal cord and locomotor activity in rats. Int J Clin Exp Pathol 6(8): 1505–1515

Motoki K, Kishi H, Hori E, Tajiri K, Nishijo H, Muraguchi A (2009) The direct excitatory effect of IL-1beta on cerebellar Purkinje cell. Biochem Biophy Res Commun 379(3):665–668

Murakami S, Takemoto T, Shimizu ZJ (1953) Pharm Soc Japan 73:1026

Nadler JV, Perry BW, Cotman CW (1978) Intraventricular kainic acid preferentially destroys hippocampal pyramidal cells. Nature 271: 676–677

Nishant PV, Joe ES (2016) Altered Cerebellar Circuitry following Thoracic Spinal Cord Injury in Adult Rats. Neural Plasticity 2016: **5 pages**.

Panegyres PK, Hughes J (1998) The neuroprotective effects of the recombinant interleukin-1 receptor antagonist rhIL-1ra after excitotoxic stimulation with kainic acid and its relationship to the amyloid precursor protein gene. J Neurol Sci 154(2):123–132

Paolicelli RC, Bolasco G, Pagani F, Maggi L, Scianni M, Panzanelli P, Giustetto M, Ferreira TA, Guiducci E, Dumas L, Ragozzino D, Gross CT (2011) Synaptic pruning by microglia is necessary for normal brain development. Science 333(6048):1456–1458

Perez SE, Chen EY, Mufson EJ (2003) Distribution of estrogen receptor alpha and beta immunoreactive profiles in the postnatal rat brain. Brain Res Dev Brain Res 145:117–139

Ritz MF, Hausmann ON (2008) Effect of 17 beta estradiol on functional outcome, release of cytokines, astrocytes reactivity, inflammatory spreading after spinal cord injury in male rats. Brain Res 1203: 177–188

Samantaray S, Sribnick EA, Das A, Thakore NP, Matzelle D, Yu SP, Ray SK, Wei L, Banik NL (2010) Neuroprotective efficacy of estrogen in experimental spinal cord injury in rats. Ann N Y Acad Sci 1199:90–94

Samantaray S, Das A, Matzelle DC, Yu SP, Wei L, Varma A, Ray SK, Banik NL (2016) Administration of low dose-estrogen attenuates persistent inflammation, promotes angiogenesis and improves locomotor function following chronic spinal cord injury in rats. J Neurochem 137(4):604–617

Shi Y, Song Y, Wang Y, Liang X, Hu Y, Guan X, Cheng J, Yang K (2009) p,p'-DDE Induces Apoptosis of Rat Sertoli Cells via a FasL-Dependent Pathway. J Biomed Biotechnol 2009: 181282

Sierra A, Azcoitia I, Garcia SL (2003) Endogenous estrogen formation is neuroprotective in model of cerebellar ataxia. J Endocrine 21:43–51

Siriphorn A, Dunham KA, Chompoopong S, Floyd CL (2012) Postinjury administration of 17beta-estradiol induces protection in the gray and white matter with associated functional recovery after cervical spinal cord injury in male rats. J Comp Neurol 520:2630–2646

Spence RD, Zhen Y, White S, Schlinger BA, Day LB (2009) Recovery of motor and cognitive function after cerebellar lesions in a songbird: role of estrogens. Eur J Neurosci 29(6):1225–1234

Sperk G (1994) Kainic acid seizures in the rat. Prog Neurobiol 42(1):1–32

Sribnick EA, Wingrave JM, Matzelle DD, Ray SK, Banik NL (2003) Estrogen as a neuroprotective agent in the treatment of spinal cord injury. Ann N Y Acad Sci 993:125–133

Sribnick EA, Samantaray S, Das A, Smith J, Matzelle DD, Ray SK, Banik NL (2010) Postinjury estrogen treatment of chronic spinal cord injury improves locomotor function in rats. J Neurosci Res 88:1738–1750

Stacey LR, Tom SO, Roy VS (2013) New roles for the cerebellum in health and disease. Front Syst Neurosci 14:7–83

Steinhäuser C, Gallo V (1996) Trends Neurosci 19:339–345

Streit WJ, Walter SA, Pennell NA (1999) Reactive microgliosis. Prog Neurobiol 57:563–581

Sua'rez I, Bodega G, Rubio M, Ferna'ndez B (1992) Sexual dimorphism in the hamster cerebellum demonstrated by glial fibrillary acidic protein (GFAP) and vimentin immunoreactivity. Glia 5:10–16

Verdaguer E, Jordá EG, Canudas AM, Dominguez E, Escubedo E, Pubill D, Camarasa J, Pallàs M, Camins A (2002) Kainic acid-induced apoptosis in cerebellar granule neurons: an attempt at cell cycle re-entry. Neuroreport 13:413–416

Wang CX, Olschowka JA, Wrathall JR (1997) Increase of interleukin-1b mRNA and protein in the spinal cord following experimental traumatic injury in the rat. Brain Res 759:190–196

Wang Q, NYu S, Simonyi A, Sun GY, Sun AY (2005) Kainic acid-mediated excitotoxicity as a model for neurodegeneration. Mol Neurobiol 31(1–3):3–16

Wolf U, Rapoport MJ, Schweizer TA (2009) Evaluating the affective component of the cerebellar cognitive affective syndrome. J Neuropsychiatry Clin Neurosci 21(3):245–253

Yang L, Andersson S, Warner M, Gustafsson JA (2001) Morphological abnormalities in the brains of estrogen receptor beta knockout mice. PNAS 98:2792–2796

Yezierski RPM, Santana SH, Madsen PW (1993) Neuronal degeneration and spinal cavitation following intraspinal injections of quisqualic acid in the rat. J Neurotrauma 10:445–456

Yuan JS, Reed A, Chen F, Stewart CN (2006) Statistical analysis of real-time PCR data. BMC Bioinformatics 22:7–85